Time domain amplitude and frequency detection of gravitational waves from coalescing binaries

L. Milano and F. Barone
Universitá di Napoli ''Federico II,'' Dipartimento di Scienze Fisiche, Mostra d'Oltremare Pad.19, I-80125 Napoli, Italy and Istituto Nazionale di Fisica Nucleare, sez. Napoli, Mostra d'Oltremare Pad.19, I-80125 Napoli, Italy

M. Milano
Universitá di Napoli ''Federico II,'' Facoltá di Ingegneria Elettronica, Via Claudio, I-80125 Napoli, Italy
(Received 26 August 1996)

We propose a multistep procedure for the on-line detection and analysis of the gravitational wave signals emitted during the coalescence of compact binaries. This procedure, based on a hierarchical strategy, consists of a rough on-line analysis of the gravitational wave signal using adaptive line enhancers filters and a fast off-line parameter estimate, using the controlled random search optimization algorithm. A more refined off-line analysis using the classic matched-filtering technique, with a greatly reduced computational burden, can follow to further improve the parameter estimate. The results of simulations for the rough analysis are quite promising both for the relatively small computational power needed and for the robustness of the algorithms used, so that it could be very helpful for gravitational wave detection with very large baseline interferometric detectors such as LIGO and VIRGO. [S0556-2821(97)05906-7]

PACS number(s): 04.40.Dg, 04.80.Nn, 95.55.Ym, 97.80.Hn

I. INTRODUCTION

Gravitational wave (GW) detection is certainly one of the most challenging goals for today's physics: a very strong proof in favor of the Einstein's general relativity description of phenomena related to the dynamics of gravitation and the opening of a completely new channel of information on astrophysical objects [1–3]. For this task, many detectors with different measurement bands and sensitivities are already operational or are planned in the world both at Earth (resonant-mass detectors [4,5], laser interferometers [6,7], etc.) and in space (spacecraft tracking [8], space interferometers [9], etc.). But, despite the great efforts produced in the last 20 years, up to now no direct evidence confirms the existence of GW's. The only credited indirect evidence of GW emission is the famous two-neutron star binary pulsar PSR 1913+16 discovered in 1975 by Hulse and Taylor [10], which is decaying due to the loss of orbital energy to gravitational waves at the rate predicted by the general relativity to better than 1% accuracy [11,12].

A real great improvement in the direction of direct GW detection will be given by the new generation of long baseline laser interferometric detectors, such as GEO [13], the Laser Interferometric Gravitational Wave Observatory (LIGO) [14], TAMA [15], and VIRGO [16], which are going to be operational at the beginning of the next century. These detectors are very promising because their projected high sensitivities, coupled to their intrinsic large measurement bands, put them in a good position for the detection of GW emitted from different classes of astrophysical objects like, for example, radiation bursts from supernovae events occurring in the Virgo cluster, periodic signals from old and new pulsars, radiation from coalescing compact binaries, stochastic background gravitational radiation, quasinormal modes of black holes, etc. [2,3].

In this paper we will focus our attention on GW signal detection from coalescing compact binaries, which seem to be very promising transient GW sources, also because of the relatively large number of expected events each year (of the order of tens per year within a few hundreds of Mpc) [17–20]. These systems are made of two compact objects [two neutron stars (NS-NS), two black holes (BH-BH), or a mixed pair (NS-BH)] spiraling very rapidly around each other in their last stage of evolution immediately preceding the final coalescence with a dynamics entirely ruled by the radiation forces due to the emission of gravitational radiation, at a frequency equal to twice the orbital frequency and the typical shape of a chirp signal [21].

As said above, the detection of GW generated by coalescing compact binary systems could be, in principle, possible with ground-based long baseline interferometric detectors, although the GW signal will probably not stand above their broadband noise. In particular, the LIGO and VIRGO antennas will be in a good position for such detection [22–26] and could provide precise measurements of the masses of the objects, of the spins and, in the case of neutron stars, of the radii [27–34].

But even if these interferometers seem to be sensitive enough for the detection of these sources, nevertheless the problem of GW signal analysis is still an open problem, whose solution requires an adequate choice of the data analysis techniques in connection with the shape of the expected signal, the noise of the detector and the available computing power [35,36].

For this task, many efforts have been made for the development of special data analysis techniques for the enhancement of the signal-to-noise ratio of these GW signals. Several algorithms have been developed and tested, but probably the best known technique is the matched-filtering technique, first suggested in this field of research by Thorne [24]. This technique, well known in communication theory as the Wiener-Komolgorov optimum filter [37,38], requires the correlation of the output of a detector with a template of the expected signal (matched filter). But, although very simple in

principle, the application of such algorithm requires a practically exact theoretical knowledge of the shape of the expected signal as function of the unknown parameters which describe the coalescing binary and, then, the correlation of the detector output with several thousands of templates. And, as it is well known, these two requirements are very difficult to satisfy for coalescing binary signals [21,39].

The shape of the GW signal can be obtained by computing the gravitational radiation field generated by a system of two point masses moving on a practically circular orbit. Actually, the solution of this problem requires the calculation of the gravitational radiation field to a very high order in terms of a post-Newtonian (PN) expansions [40], because coalescing compact binaries are strongly dominated by relativistic effects [22–24]. This radiation field has been calculated up to the PN2 approximation [41–43], although recently the precision of the energy loss has been extended to include the next PN2.5 approximation [44]. But, although the PN2 precision is still insufficient to make full use of the phase data [45,46], the PN2 waveform amplitude is close to the needs of the LIGO and VIRGO detectors [30–32]. For this task, analytic expressions have been obtained in a form directly usable for GW data analysis by [47].

The large number of templates necessary for data analysis using matched-filtering technique raises problems due to the great computing power needed for performing this task on line [21,35,36]. In fact, as a consequence of the large band of these detectors (some kHz) sampling rates of the order of 20 kHz are foreseen, resulting in a huge amount of data/day to be analyzed on line (of the order of 10 GByte/day). Of course, the analysis of such a large amount of information could be made off line, but it would be better to select on line all the data frames which may contain a GW signal.

At this stage, two are the most credited approaches to solve this problem. The first approach consists in defining a single-step procedure characterized by a full on-line fine analysis of the data with selection of the signals and determination of the coalescing binaries parameters (matched filters) while the second approach consists in a hierarchic procedure characterized by a rough analysis for the selection of frames of data which could contain GW signals with a reasonable degree of confidence (adaptive filters, optimization algorithms, matched filters, etc.) followed by a fine analysis with more refined techniques (matched filters).

Actually, the direct application of the matched-filtering technique to the VIRGO antenna requires a computing power of about $20-30$ GFlops at the lowest post-Newtonian order (PN0) and about 80 GFlops at the first post-Newtonian correction (PN1) in order to recover 95% of the SNR, including the computing power necessary for the production of the templates [48]. An analogous prediction for the LIGO antenna gives substantially comparable results [49]. These estimates confirm that already at the stage of the first post-Newtonian correction large parallel computers are necessary for the on-line analysis of these signals. Moreover, even if we assume an easily available computing power, the matched-filtering technique raises problems due to the filters computational complexity coupled with their lack of robustness in connection with possible signal missing or the change of the statistics of the signal due the presence of nonstationary noise. Moreover, but not secondary, the performances of a matched filter strongly degradate if the theoretically predicted signal is not close to the real one.

In order to solve these theoretical problems and to reduce the large amount of computing power required for such analysis, some algorithms have been proposed, like, for example, the algorithm proposed by Smith [50] for real-time detection of coalescing binary waveforms, which requires resampling the data stream at increasingly larger rate in order to compensate the increase in frequency of the signal. When the signal is present, the Fourier transform of the resampled data will peak at a particular frequency, which depends on how fast the data are resampled. The rate at which the resampling is done is the same for all the waveforms, whose frequencies remain proportional to each other until the coalescence time. This method has the advantage that a simple Fourier transform will pick up the signal, but it does not help in saving computing time, because of the resampling data needed for every time of arrival [21].

Probably, the best way to solve this problem is to use the hierarchical strategy, first performing an on-line rough analysis of the signal in order to select all the possible data frames which could contain a signal, followed by a finer off-line search using more refined techniques. A possible solution for the application of the matched-filtering technique in a hierarchical search could be that of using a corresponding lower threshold at a first stage, then refining the analysis in correspondence of signal crossing the first threshold, using more finely spaced templates and also more refined formulas. This solution proposed by Thorne [35,36] would decrease the computing power needed of a factor 10. Other possible proposed strategies could be those of performing searches using genetic algorithms or global optimization with simulated annealing [49] or the hierarchical strategies like the one proposed by Mohanty and Dhurandhar [51].

A hierarchic strategy is foreseen also for the VIRGO antenna [16]. In fact, all the data, collected and stored in frames by a Frame Builder, will be analyzed on line by to-be-defined on-line algorithms which will select all the frames in which a GW signal could be present. All the selected frames will then be archived by the on-line data distribution system on disks (an amount of 500 GByte is foreseen for the on-line storage) and on tapes [DST (data summary tapes)] for a refined off-line analysis. Nevertheless, all the frames, selected or not, will be archived by a raw data archiving system on tapes in order to allow a full off-line processing [16,52,53].

Also we think that a hierarchical strategy is probably the best way of overcoming this problem. Within this framework, we have developed an on-line hierarchical strategy whose main goal is that of saving computing power and leaving the necessary uncertainty margin between the theoretically predicted signals and the experimental ones, without degrading the performances of the data analysis algorithms.

The strategy we propose for the rough analysis consists in dividing the problem of filtering into two steps, in order to obtain separate information on the amplitude and frequency of the signal, instead of doing everything at the same time [54,55]. For this task, we tested an adaptive noise cancelling algorithm of the class of adaptive line enhancers (ALE's) [56]. In fact, the signal to be detected is a classic modulated signal which exhibits at the same time the three basic forms of modulation in amplitude, frequency and phase. In particu-

lar, the modulation in amplitude is related only with the physical and geometrical structure of the source, while the frequency and phase modulations are related also to effects which depend on the relative position of the detectors with respect to the source. Therefore, a multistep on-line procedure can be defined as (1) **1° step**, rough analysis of interesting sequences of a GW antenna output data with suitable algorithms (adaptive filters); (2) **2° step**, suitable refined off-line data analysis with more powerful but computationally more complex algorithms (global optimization algorithms and matched filters).

In particular, the rough analysis must be efficient and robust, with the following characteristics: (1) minimum loss of signals which can be extracted from refined algorithms; (2) robustness against false alarm detection like the refined ones.

As we shall show in this paper, we succeed in getting an almost complete rough characterization of the signals we are interested in, estimating the mass parameter, coalescing duration and distance in the case of optimal orientation source-antenna of the simulated binary coalescence at the Newtonian order. Tests were also performed at the first post-Newtonian order and the results we got have shown that the performances of the algorithm we implemented are fairly good also for PN1 terms. For this work we have used the chirp waveforms derived by Krolak (1989) [28] and adapted for numerical computations by Verkindt (1993) [57]. In a following paper we shall test the most up-to-date chirp waveforms up to the 2.5 post-Newtonian order and we shall use more realistic noise constraints.

II. GW SIGNAL FROM COALESCING BINARIES

In this section we briefly describe the nature of the gravitational wave form emitted by a coalescing binary system. As is well known, in the transverse traceless (TT) gauge, the gravitational wave emitted by a system is described in terms of the two polarizations usually denoted by $h_+(t)$ and $h_\times(t)$ [1]. According to this terminology the noise-free response of the detector is simply given by [58,59]

$$R(t)=F_+h_+(t)+F_\times h_\times(t), \tag{2.1}$$

where F_+ and $F_\times$ are functions of the angles describing the orientation of the detector and the position of the source, $h_+(t)$ and $h_\times(t)$ are expressed by

$$h_+(t)=h(t)(1+\cos^2 i)\cos\left[2\pi\int f(t)dt+\phi\right], \tag{2.2}$$

$$h_\times(t)=2h(t)\cos i\times\sin\left[2\pi\int f(t)dt+\phi\right], \tag{2.3}$$

where i is the inclination of the orbital plane, and $h(t)$ is the amplitude of the gravitational signal at the detector level

$$h(t)=\left[\frac{2\mu G}{dc^4}\right][GM\pi f(t)]^{2/3}, \tag{2.4}$$

where μ and M are the reduced and total mass of the binary, respectively, d is the distance from Earth, $f(t)$ is the instantaneous frequency of the gravitational wave, and ϕ is the phase of the wave at some fiducial frequency. In particular, the time dependence of the phase and of the frequency of the radiation and the total number of revolutions done by the binary can be expressed as

$$\chi(t)=\frac{8}{5}\tau\left[1-\frac{t}{\tau}\right]^{5/8}, \tag{2.5}$$

$$f(t)=f_0\left[1-\frac{t}{\tau}\right]^{-3/8}, \tag{2.6}$$

$$N=\frac{1}{32}\pi^{-8/3}\frac{c^5}{G^{5/3}}K^{-1}f_0^{-5/3}, \tag{2.7}$$

where $K=\mu M^{2/3}$ and τ is the time lacking to the coalescence, if no tidal disruption occurs, when the GW frequency is equal to f_0,

$$\tau=\frac{5\pi^{-8/3}}{256}\frac{c^5}{G^{5/3}}\frac{1}{K}f_0^{-8/3}. \tag{2.8}$$

Using Eq. (2.1), the response of the detector can be written as

$$R(t)=h(t)[F_+^2(1+\cos^2 i)^2+4F_\times^2\cos^2 i]^{1/2}\times\cos\left[2\pi\int f(t)dt+\psi+\phi\right], \tag{2.9}$$

where

$$\psi=\arctan\left[\frac{2F_\times\cos i}{F_+(1+\cos^2 i)}\right]. \tag{2.10}$$

These expressions show that the only effect of any arbitrary orientation of the detector with respect to the plane of the orbit of the binary is that of changing the amplitude and the phase of the output signal without affecting its time dependence. On the basis of what is said above and without loss of generality, the noise-free response of the detector to the signal can be rewritten in a more convenient way as

$$s(t)=kHh(t)\cos[2\pi f(t)t+\phi_0], \tag{2.11}$$

$$h(t)=2.56\times10^{-21}\left[\frac{K}{M_\odot^{5/3}}\right]\left[\frac{\mathrm{Mpc}}{d}\right]\left[\frac{f(t)}{100\ \mathrm{Hz}}\right]^{2/3}, \tag{2.12}$$

$$\left[\frac{f(t)}{100\ \mathrm{Hz}}\right]=\left(\left[\frac{f_0}{100\ \mathrm{Hz}}\right]^{-8/3}-0.332\left[\frac{K}{M_\odot^{5/3}}\right]t\right)^{-3/8}, \tag{2.13}$$

$$\tau=3.0\left[\frac{f_0}{100\ \mathrm{Hz}}\right]^{-8/3}\left[\frac{K}{M_\odot^{5/3}}\right]^{-1}, \tag{2.14}$$

$$N=480.0\left[\frac{K}{M_\odot^{5/3}}\right]^{-1}\left[\frac{f_0}{100\ \mathrm{Hz}}\right]^{-5/3}, \tag{2.15}$$

where $K=\mu M^{2/3}$, $\mathcal{M}=K^{3/5}$ is the so-called chirp mass, and d is the distance in Megaparsecs (Mpc) (the masses are expressed in solar units). Finally, the parameter kH $(0<kH<1)$ depends on the source-detector orientation (in our simulation we assumed $kH=1$). As it is easy to see,

this signal has the typical structure of an amplitude modulated signal, $h(t)$, with a time dependent carrier, $f(t)$, and a starting phase ϕ_0 and is valid in the hypothesis in which tidal effects, post-Newtonian correction, Doppler shift, and orbital eccentricity are neglected. The detection of this signal simply implies the determination of these quantities. In particular, the amplitude modulation is only related to the physical and geometrical structure of the source, while the frequency and phase modulations are related also to effects which depend on the relative position of the detectors with respect to the source.

At the final stage of the coalescence, when the post-Newtonian terms of the development in v/c must be taken into account, the following first order post-Newtonian corrections to the amplitude and phase of the signal, respectively, must be introduced [57]:

$$\mathrm{PN1}_h(t) = 4.04\times 10^{-24}\frac{1}{d}\left(1-0.514\frac{\mu}{M}\right)\mu^{-1}f(t)^{4/3}, \tag{2.16}$$

$$\mathrm{PN1}_\phi(t) = 1.5\times 10^{4}\left(1+1.24\frac{\mu}{M}\right)\mu^{-1}f(t)^{-1}. \tag{2.17}$$

Taking into account these terms, we performed some simulations in order to test the performances of the algorithms also at the PN1 order.

III. ALGORITHMS FOR SIGNAL EXTRACTION

As we stated above, one of the most credited algorithms for the gravitational signal extraction from the noise due to the detector is the matched-filter technique, whose theory, for sake of completeness, we briefly recall here [37,38]. The purpose of this filter is to extract the signal with the constraint of maximizing the signal-to-noise ratio. For this task, if we assume a signal, $s(t)$, buried in noise, $n(t)$, then the detector output signal can be written in the linear case as

$$s_{\mathrm{out}}(t) = s(t) + n(t). \tag{3.1}$$

Therefore, if the Fourier transform of the signal is $\tilde{s}(f)$, then any stationary linear operation on the output can be expressed as a convolution of the signal with a filter $q(t)$, that is

$$c(t) = s_{\mathrm{out}}(t) * q(t) = \int_{-\infty}^{\infty} s_{\mathrm{out}}(\tau)q(\tau+t)d\tau$$

$$= \int_{-\infty}^{\infty} \tilde{s}_{\mathrm{out}}(f)\tilde{q}^{\star}(f)e^{2\pi i f t}df. \tag{3.2}$$

Computing the expectation value of the filter output, assuming a Gaussian noise, $n(t)$, and evaluating its variance, we get a *raw* signal-to-noise ratio, which is possible to maximize by means of a suitable choice of the filter $q(t)$. If the output contains a signal, this filter gives an amplitude signal-to-noise ratio (SNR) in $c(t)$ (ratio of maximum value to the standard deviation of the noise) expressed by

$$(\mathrm{SNR})^2_{\mathrm{opt}} = 2\int_0^{\infty}\frac{|\tilde{h}(f)|^2}{S_h(f)}df. \tag{3.3}$$

As is well known from the theory, this is the largest SNR achievable with a linear filter and, in the case of Gaussian noise, this is also the largest possible SNR ratio [2]. Therefore, one might think that by performing a filtering of the incoming data stream with many independent filters, one would just find the filter that gives the best correlation with the signal and then infer the mass parameter, phase, amplitude, and time-of-arrival from that. But when we search for coalescing binary signals, obviously, we do not know the value of the mass parameter K: we have a range of physically meaningful mass parameters spanning from 0.25 up to 50 at the zero Newtonian order. In other words, there are some weak points in the matched-filtering procedure which cannot be ignored: an almost exact knowledge of the shape of the signal is needed; the exact shape of the noise must be known; a large number of filters (thousands) are necessary to detect the signal, if any is present, because the mass parameter is unknown; post-Newtonian terms can lead to a mismatching of the signal after few cycles; an optimal threshold must be established in order to minimize the false alarm probability according to the hypothesis of stationarity of the noise.

Summing up, we need a lot of templates for the signal and we can hope to solve these problems only using on-line parallel computers. Starting from this kind of trouble, as stated in the Introduction, we searched for different algorithms which, notwithstanding their suboptimality, can be more suitable for a real-time on-line rough analysis than the matched filters. In particular, we searched for algorithms which allowed us to split the problem of filtering into two parts in order to obtain separate information on the amplitude and frequency of the signal, instead of doing everything at the same time. To satisfy these requirements we tested adaptive algorithms of the class of adaptive line enhancers (ALE's) [60], which, notwithstanding their suboptimality, are faster and computationally lighter than the matched-filtering ones.

IV. ADAPTIVE LINE ENHANCERS (ALE's)

The algorithms we tested for the on-line detection of coalescing binaries belong to the class of the partially adaptive filters used to obtain a time-frequency output from the filtered signals. For this task we modified a classical filter we used for tracking of signals in additive white Gaussian noise (AWGN) in order to obtain the characterization of the frequency of the input signal or the amplitude determination in the *time domain*. The adaptive filter we tested is a classical IIR based adaptive line enhancer (ALE) filter, designed in such a way to be only partially adaptive for it works in a constrained recursive center frequency adaptive configuration for the enhancement of noisy bandpass signals, which allows one to vary only its center frequency [56].

A. The adaptive line enhancer

An interesting approach to the problem of signal extraction from noise is represented by an adaptive line enhancement of the input signal. For this task, many different methods have been developed, which can be classified into two main categories: finite impulse response (FIR) and infinite impulse response (IIR) based methods [61].

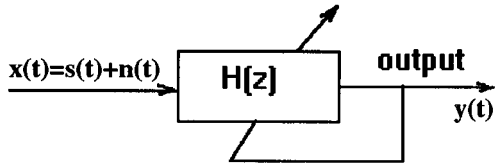

$$PF = E\left[y^2(t)\right] = \frac{1}{2\pi j}\oint \left|H(z)\right|^2 \Phi_{xx}(z)\frac{dz}{z}$$

FIG. 1. Scheme of the recursive center-frequency adaptive filter we used for chirp tracking and cost function PF to be maximized.

In FIR based methods, the signal is modeled like an autoregressive (AR) process, whose parameters are estimated using, for example, the least mean square (LMS) algorithm [60,62–64]. Although this approach has the advantage of producing stable filters, it is computationally expensive if good accuracy is required. On the other hand, the computation time of the IIR based methods is reduced at the expense of taking care of some instability problems. But what is worth noticing is that both models are well suited for stationary signals and, what is really interesting, in some cases they can enhance one or more narrowband signals of unknown and possibly drifting amplitudes and frequencies which are embedded in broadband noise [65].

Taking into account our need of a robust and fast algorithm for on-line signal detection and tracking in noise we tested a simplified version of the ALE filter aimed at the processing of signals embedded in additive Gaussian noise with zero mean and variance σ^2 [56]. The procedure we applied is based on the implementation of a center-frequency adaptive filter with the constraint of a constant bandwidth and with the allowance of the variation of the center frequency of the filter by changing of its dependent coefficients. Therefore, the transfer function and order of the filter can be designed according to the *a priori information* (not exact knowledge) of the type and bandwidth of the input signal and the out-of band noise requirements.

In the following we will discuss the structure of the ALE adaptation mechanism, showing and discussing the structure of the filter. In particular, we implemented the system basing its adapting response to the performance criterion of maximizing the mean-squares output of the bandpass filter as shown in Fig. 1.

It is well known that for an input of a bandpass signal in AWGN, the resulting function will be normally unimodal with the peak occurring at the best solution for the coefficients, for which the filter center frequency is equal to the center frequency of the bandpass input. A recursive maximum-mean-squares algorithm was implemented starting from the transfer function of a recursive digital filter of order 2 in the z domain,

$$H(z) = \frac{a_0 + \Sigma_{i=1}^{2} a_i z^{-i}}{1 + \Sigma_{i=1}^{2} b_i z^{-i}}, \tag{4.1}$$

assuming as a performance function

$$PF = E[y^2(t)] = \max, \tag{4.2}$$

where $y(t)$ is the output of $H(z)$ for an input $x(t)$ as shown in Fig. 1. Being the objective of this algorithm, the maximization of PF within the region of stability, the filter coefficients a_i and b_i *depend only on one parameter: the central frequency of the filter* and can be updated with increments proportional to the instantaneous gradient. Since this algorithm maximizes the mean-squares output, it yields stable parameter estimates only for severe and computationally complex stability constraints. Hence, this algorithm may be insufficient for the implementation of general adaptive filters. However, it yields stable parameter estimates in the case of the center frequency adaptive filters for a large range of its *scalar* convergence parameter, μ_a.

According to [56], we implemented the constrained ALE second-order bandpass Butterworth filter with

$$H(z) = (1-r^2)\left[\frac{W_t z/(r+r^2) - 1}{z^2 - W_t z + r^2}\right], \tag{4.3}$$

where $W_t = 2r\cos\omega_0$ is the only center-frequency (ω_0) parameter-dependent term, while r is a fixed design parameter related to the normalized filter bandwidth B, by the relation $B = \pi(1-r)$. The stability of this filter requires that $|W_t| < 2r$. Since the objective of the filter is to tune the signal, then the optimum value of W_t is $W_{0_p} = 2r\cos\omega_{0_p}$ where ω_{0_p} is the normalized angular center frequency of the input. From $W_{0_p} = 2r\cos\omega_{0_p}$ we can derive the tracked frequency, $f_0(t)$, of the signal along the time

$$f_{0_p}(t) = f_s \times a\cos\left(\frac{W_{0_p}}{4\pi r}\right), \tag{4.4}$$

where f_s is the sampling frequency. Therefore, using Eq. (4.4), the recursive algorithm for the filter can be expressed by

$$y_t = W_t\left(\frac{1-r}{r}\right)x_{t-1} - (1-r^2)x_{t-2} + W_t y_{t-1} - r^2 y_{t-2}, \tag{4.5}$$

$$\alpha_t = \frac{\delta y_t}{\delta W_t} = \left(\frac{1-r}{r}\right)x_{t-1} + W_t\alpha_{t-1} + y_{t-1} - r^2\alpha_{t-2}, \tag{4.6}$$

$$W_{t+1} = W_t + \mu_a y_t \alpha_t / R_{t+1}, \tag{4.7}$$

$$R_{t+1} = \nu R_t + \alpha_t^2 \quad (0 < \nu < 1), \tag{4.8}$$

where ν is the scalar *forgetting factor*, introduced for the recursive computation of the normalizing factor R for the instantaneous gradient α_t, and μ_a is the scalar adaptation step size. Because of the small number (typically one in our case) of adapting coefficients, stability monitoring of these filters is very simple, being performed in order to verify the condition $|W_t| < 2r$. Concerning the computational efficiency of recursive adaptive filters, it is well known that it largely depends on the number of unknown coefficients. Since these filters have few coefficients, they are computationally very efficient compared to the completely adaptive filters. More-

over, if we take into account the availability of a large gradient in the vicinity of the optimum of the performance function, the algorithm exhibits faster convergence compared to the completely adaptive filters, expecially while it closely tracks the signal [56].

V. ANALYSIS OF ALE PERFORMANCES

The center-frequency adaptive filters continuously track the center frequency of the input signal and tune to it when the input is temporarily stationary in center frequency. When tuned to the center frequency of the input, an adaptive filter yields maximum SNR improvement:

$$I=\left(\frac{\mathrm{SNR_{out}}}{\mathrm{SNR_{in}}}\right)^{\star}=\left(\frac{(1/2\pi j)\int|H(z)^{\star}|^2\Phi_{ss}(dz/z)}{(1/2\pi j)\int|H(z)^{\star}|^2\Phi_{nn}(dz/z)}\right)\Bigg/\ \mathrm{SNR_{in}}, \tag{5.1}$$

where $H(z)^{\star}$ is the transfer function of the filter when tuned to the input signal, and Φ_{ss} and Φ_{nn} are the power spectral densities of the input signal and noise components, respectively. Assuming AWGN in input we can further write

$$I=\frac{(1/2\pi i)\int|H(z)^{\star}|^2\Phi_{ss}(dz/z)}{\sigma^2 B_{\mathrm{eq}}}\Bigg/\ \mathrm{SNR_{in}}, \tag{5.2}$$

where σ^2 is the input one-sided power spectral density or noise power and B_{eq} is the equivalent noise bandwidth. B_{eq} can be evaluated from

$$B_{\mathrm{eq}}=\frac{1}{2\pi j}\int|H(z)^{\star}|^2\frac{dz}{z} \tag{5.3}$$

using the residue method.

Therefore, if we assume that $(1-r)\ll 1$ and that the filter is closely tracking the signal, we can state that for the second-order bandpass Butterworth filter like ALE it is possible to obtain an improvement of the optimum SNR as

$$I\approx\frac{1+r}{2(1-r)}. \tag{5.4}$$

At this point it is necessary to discuss how to implement a trigger and the criterion of choice of the threshold T, according to which we can discriminate between the alternative hypotheses of absence or presence of a signal at an assigned level of confidence. In this discussion we will show that the performances of the implemented ALE filters tend to approximate those of a matched filter and, of course, are not better than them. This point, as we shall see, is related to the choice of the optimum threshold for the trigger. Let us suppose to implement a matched-filter-based trigger assuming: additive white Gaussian noise (AWGN, of PSD σ^2), the form of the signal is exactly known, and the ALE filter tracks exactly the signal.

The first hypothesis is necessary because our implementation of the ALE filter works in AGWN and, therefore, it is a natural choice to assume the same noise environment to compare the performances of the two algorithms. The second hypothesis is necessary to define the best situation for the matched filter, i.e., it is supposed to be perfectly tuned to the signal in order to obtain the maximum output peak. The third hypothesis is equivalent to the second one, but for an ALE filter. Let $s(t)$ be the input signal, $S(f)$ its Fourier transform, $n(t)$ a noise process satisfying the hypothesis. The matched-filter transfer function must, by definition, maximize the filter output SNR, i.e.,

$$K(t):\mathrm{SNR_{out}}\mathrm{max!}, \tag{5.5}$$

where $K(t)$ is the filter impulse response, and $\mathrm{SNR_{out}}$ can be derived considering the input signal

$$x(t)=s(t)+n(t) \tag{5.6}$$

and the corresponding output of the matched filter

$$y(t)=K(t)*s(t)+K(t)*n(t)\equiv s'(t)+n'(t). \tag{5.7}$$

Therefore, the output $\mathrm{SNR^2_{out}}$ of the matched filter can be written as

$$\mathrm{SNR^2_{out}}=\frac{S(t_0)^2}{VAR(n)} \tag{5.8}$$

at a certain time t_0.

It is well known that the optimum $K(f)$, in the way specified by the condition on $K(t)$, is expressed by

$$K(f)=Ce^{-2\pi f t_0}\frac{S^*(f)}{\sigma_n^2} \tag{5.9}$$

(C can be unitary without loss of generality). Therefore, the optimum $\mathrm{SNR^2_{out}}$ is

$$(\mathrm{SNR}^M_{\mathrm{out}})^2=\frac{1}{\sigma_n^2}\int_0^{\infty}|S(f)|^2df=\frac{\mathcal{E}_S}{\sigma_n^2}, \tag{5.10}$$

where $\mathcal{E}_S$ is the energy of the input signal $s(t)$. The trigger is implemented considering a set of signal templates and the corresponding matched filter set, the input signal is processed by all the filters and the output of the one yielding the maximum $\mathrm{SNR_{max}}$ is considered. The $\mathrm{SNR_{max}}$ is compared with a threshold T, chosen in order to give an error probability of one false alarm per year. If $\mathrm{SNR}^M_{\mathrm{max}}>T$ then it is assumed that a signal is present. Further analysis can be done, with a more restricted, but more refined in resolution, set of templates. Let us now turn our attention to the ALE filter. We recall the fact that it is a second-order Butterworth bandpass filter, whose center frequency is the only parameter that is recursively adapted, while its normalized bandwidth, $B=\pi(1-r)$, is a design parameter depending on r. In other words the filter is not *fully adaptive*. According to the hypotheses we made, the output power can be written as

$$E[y^2(t)]\cong S(f)|H(e^{j2\pi f})|^2+\sigma_n^2\frac{1-r}{1+r},\quad (1-r)\ll 1, \tag{5.11}$$

where $f=f(t)$ is the signal instantaneous frequency and $S(f)$ is the signal instantaneous amplitude. According to the third hypothesis, ALE tracks the input signal, therefore implying that the filter center frequency tends to the signal instantaneous frequency, giving in this way an estimate of this frequency. If the third hypothesis is valid, the

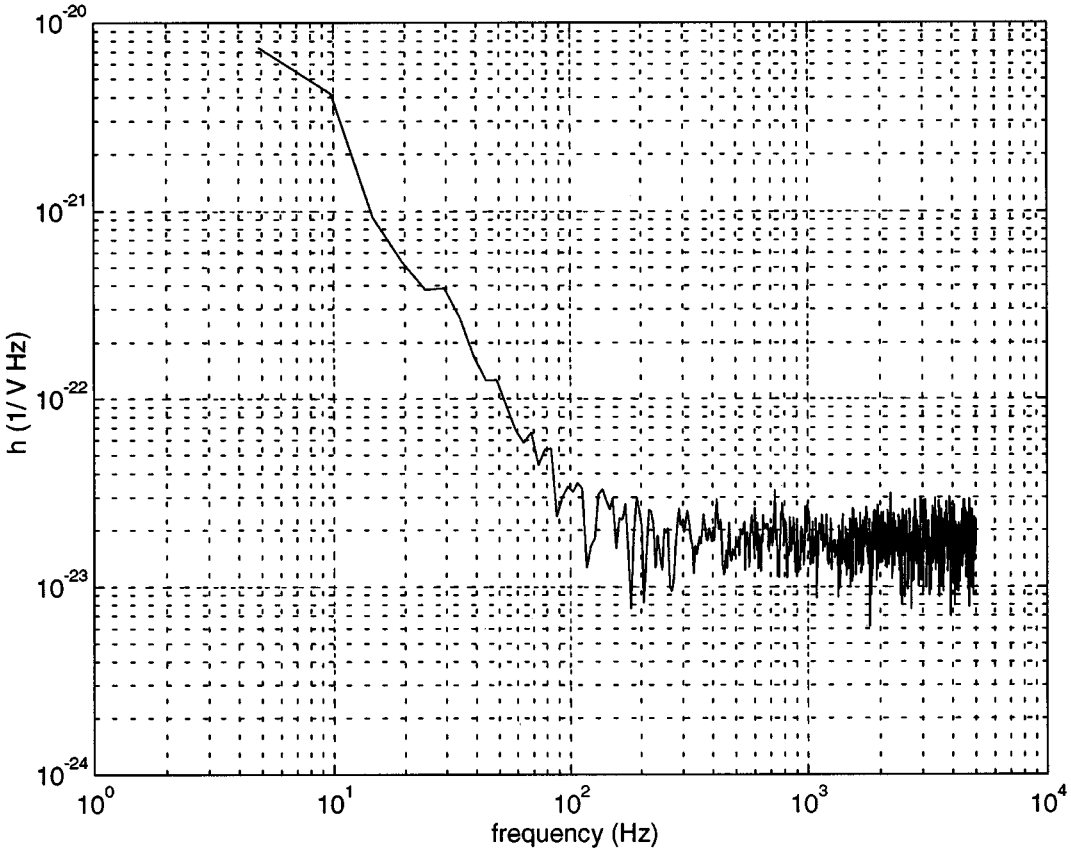

FIG. 2. Simplified sensitivity curve of VIRGO interferometric GW antenna. In this curve only the low frequency thermal pendular noise and the shot noise are taken into account.

$|H(e^{j2\pi f})|^2$ tends to be unitary in correspondence to the signal instantaneous frequency. This implies that it is possible to write the $\mathrm{SNR}_{\mathrm{out}}^{\mathrm{ALE}}$ for ALE in the following way:

$$\mathrm{SNR}_{\mathrm{out}}^{\mathrm{ALE}} \equiv \frac{\mathcal{E}_s}{\sigma_n^2} \times \frac{1+r}{1-r} = \mathrm{SNR}_{\mathrm{out}}^{M} \times \frac{1+r}{2(1-r)}. \quad (5.12)$$

This result *must not* be interpreted saying that an ALE is $(1+r)/2(1-r)$ times better than a matched filter, because the output of a matched filter is a quantity expressing the correlation between the filter template and the input, while the output of ALE is the input signal, that, if closely tracked, is left unaltered, plus a noise of standard deviation σ_{out}, much lower than the input noise. Therefore, Eq. (5.12) simply states that an ALE can achieve an improvement of the signal-to-noise ratio of the input signal. A matched-filter trigger could be used at the output of an ALE filter to obtain optimum performances for the trigger. Of course, the cause of the apparently better performances obtained with the

TABLE I. The systems were chosen to cover the known range of mass parameter, $\mathcal{M}$. In the table the headings refer to the component type of the coalescing system, the masses of the objects, the theoretical mass parameter, $\mathcal{M}_t$ the starting theoretical frequency, f_{o_t}, considered in the simulation, the theoretical duration, τ_t, of the coalescence in sec, the theoretical distance, d_t, in Mpc; the corresponding estimates obtained from the analysis are shown with their standard errors with indexes m.

Numerical tests with ALE									
System		Theoretical values				Measured values			
Type	$m_1+m_2(M_\odot)$	$\mathcal{M}_t(M_\odot)$	f_{o_t} (Hz)	τ_t (sec)	d_t (Mpc)	$\mathcal{M}_m(M_\odot)$	f_{o_m} (Hz)	τ_m (sec)	d_m (Mpc)
NS-NS	0.5+0.5	0.44	100	12.12	100	0.59±0.07	84±6	11.99±0.10	90±6
NS-NS	1.4+1.4	1.21	100	2.15	100	1.2±0.1	103±5	1.80±0.30	90±10
NS-NS	1.4+1.4	1.21	100	2.15	500	1.3±0.1	100±5	1.80±0.30	300±40
NS-BH	1.4+5.0	2.22	100	0.75	500	2.23±0.04	99±1	0.76±0.05	500±100
NS-BH	1.4+10.0	2.99	100	0.49	500	3.00±0.04	99.2±0.7	0.46±0.02	510±70
BH-BH	5.0+5.0	4.35	100	0.26	500	4.12±0.04	100.3±0.6	0.24±0.02	470±60
BH-BH	5.0+10.0	6.09	100	0.15	500	5.70±0.03	99.0±0.2	0.15±0.02	490±70
BH-BH	10.0+10.0	8.70	100	0.082	500	7.72±0.03	96.9±0.2	0.08±0.02	500±100

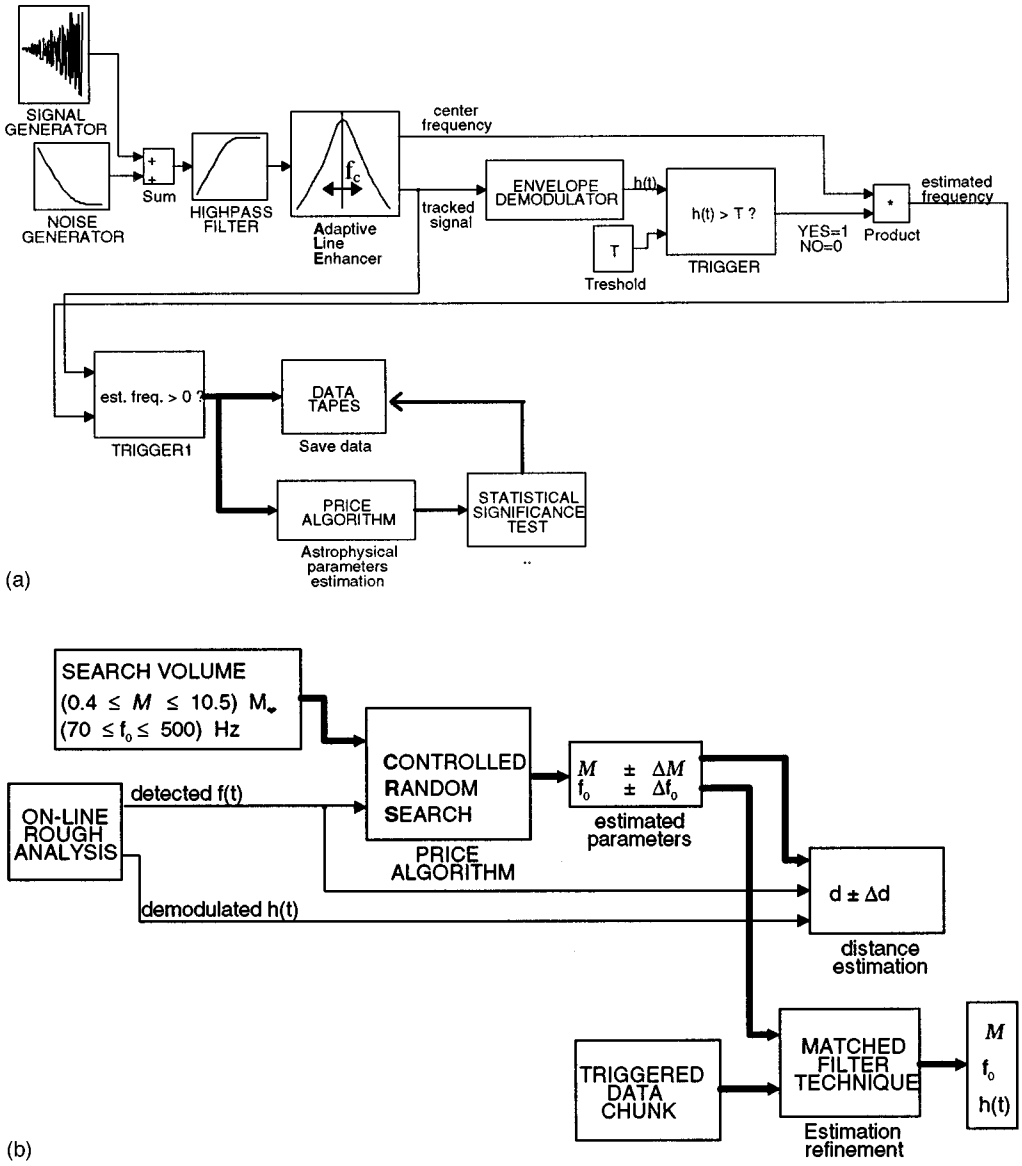

FIG. 3. (a) Scheme of the whole procedure of detection and analysis we implemented; (b) scheme of the procedure of analysis we implemented to get rough estimates of astrophysical parameters of the coalescence.

simple trigger implemented in this work than the one of a matched filter are due to the different noise environment of the ALE output.

VI. RESULTS OF THE SIMULATIONS

To test the conditions of efficiency and robustness of the implemented algorithm, we simulated a simplified output sensitivity response of VIRGO antenna between 1 Hz up to 5 KHz taking account the two main sources of noise in VIRGO, i.e., the low frequency thermal pendular noise and the high frequency shot noise according to the following specifications [16,57] (see Fig. 2):

$$|\widetilde{\mathrm{SNR}}(f)|^2=\left(\frac{a_t}{f^2}\right)^2+a_s^2 \ \ \mathrm{Hz}^{-1}, \tag{6.1}$$

where a_t, related to the pendular thermal noise, was assumed equal to 2×10^{-19} and a_s, related to the shot noise, was assumed equal to 2×10^{-23}.

All the simulations were performed in additive prewhitened Gaussian noise (APWGN) of different spectral linear densities: (1) $\tilde{h}=2\times10^{-21}$ Hz$^{-1/2}$ at 100 Hz (worst case); (2) $\tilde{h}=2\times10^{-23}$ Hz$^{-1/2}$ at 100 Hz (best case), in order to take account both the foreseen different sensitivities of VIRGO antenna at different stages of its implementation [16].

We performed some tests on the system shown in Table I according to both the worst and the best sensitivity cases for VIRGO. We shall discuss the results in the next section.

For what concerns the problem of the optimum threshold for the implemented trigger, from the discussion of the previous section on ALE performances the following criteria can be assumed. The demodulator output power, if only noise is present, can be modeled by a random variable hav-

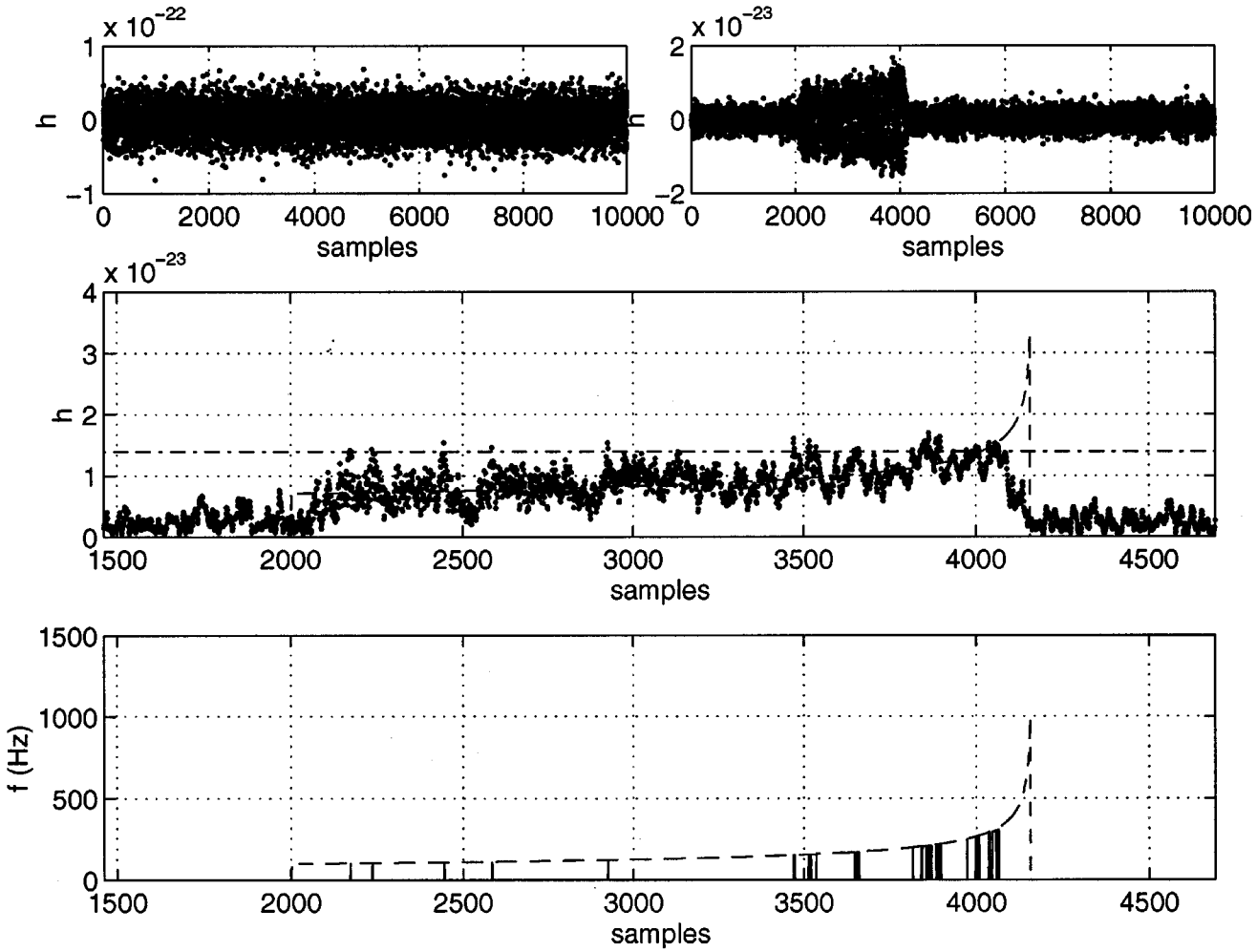

FIG. 4. From the top to the bottom clockwise: the GW input signal buried in noise, emitted by the classical NS-NS coalescing binary system of $(1.4-1.4M_{\odot})$ and coming from a distance of 500 Mpc (SNR≈ -3 dB) is shown. On the top right the output signal from ALE is shown. It is possible to see the great improvement of the $\mathrm{SNR}_{\mathrm{out}}$ that reach the value of $\approx +8$ dB. In the middle are shown the demodulated amplitude (dots), the theoretical one (continuous line, application time of the signal $2s$) and the threshold (dashed line). On the bottom the detected frequencies (bars) and the theoretical frequency trend (dashed line) are shown.

ing a Rayleigh distribution, with variance $2(1-r)/(1+r)\sigma_n^2 \equiv \sigma_N^2$. If a signal is present and is tracked, the output power statistic becomes a *Rician* distribution, with mean $\mathcal{E}$ and variance σ_N^2. The error probability, assuming independent samples, can be written as

$$\begin{aligned} P_e &= P(\text{noise} > T) \times P(\text{noise only}) \\ &\quad + P[(\text{signal}+\text{noise}) < T] \times P(\text{signal}) \\ &= e^{-T^2/2\sigma_N^2}(1-P_s) + P[(\text{signal}+\text{noise}) < T] \times P_s , \end{aligned} \tag{6.2}$$

where P_s is the probability of a signal to be present that is very low.

Because of the fact that $P_s \ll 1$, P_e can be conveniently bounded as

$$P_e \leqslant 2e^{-T^2/2\sigma_N^2} \tag{6.3}$$

so giving a closed form for the optimum threshold T:

$$T \geqslant \sigma_n \sqrt{-\frac{4(r-1)}{r+1} \ln \frac{P_e}{2}}. \tag{6.4}$$

In this work we assume $P_e \cong 10^{-12}$ (corresponding to 1 false alarm probability per year) and with $r=0.99$ and $\sigma_n = 2\times 10^{-23}$ Hz$^{-1/2}$. We obtained a threshold, $T \cong 1.5\times 10^{-23}$, for the demodulated amplitude $h(t)$.

We want to stress that this fact is the direct consequence of the enhancement of the SNR performed by ALE which allowed us to assume a threshold T for the output $\sqrt{I}$ times smaller than the one necessary for the input signal.

We tested the performances of the algorithm we are dealing with, using the systems of Table I and implementing the procedure outlined in Fig. 3. In Figs. 4–6 examples are shown of the detected frequencies and demodulated amplitudes of some simulated signals in the time domain (full line) and the theoretical trend of the amplitudes and frequencies (dashed lines) at the Newtonian order along the time of the coalescing systems emitting GW. We also performed some experimental tests on simulated data to verify the rejection factor on the data extraction obtaining, using an Alpha Vax,

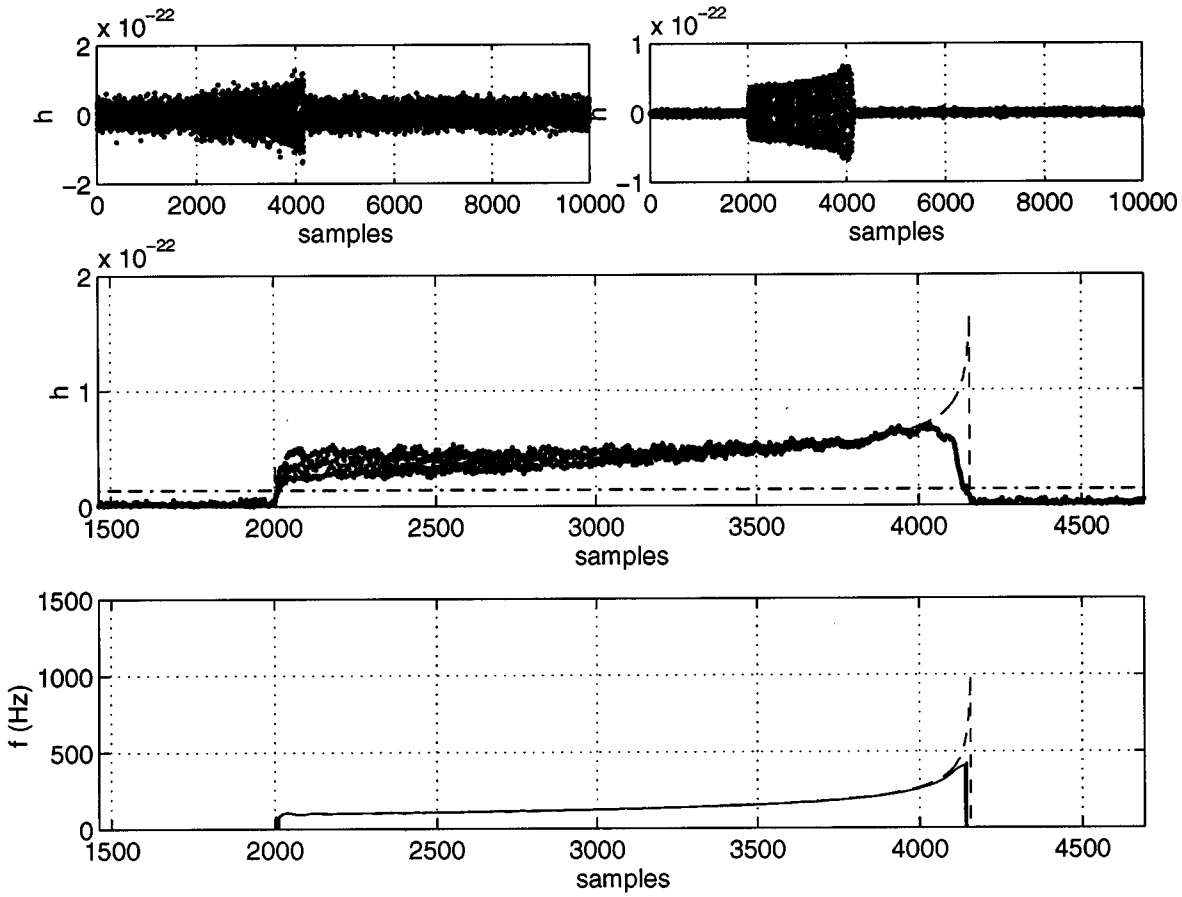

FIG. 5. From the top to the bottom clockwise: the GW input signal buried in noise, emitted by the classical NS-NS coalescing binary system of $(1.4-1.4M_{\odot})$ and coming from a distance of 100 Mpc (SNR$\approx+5$ dB) is shown. On the top right the output signal from ALE is shown. It is possible to see the great improvement of the $\mathrm{SNR}_{\mathrm{out}}$ that reach the value of $\approx+15$ dB. In the middle are shown the demodulated amplitude (dots), the theoretical one (continuous line, application time of the signal $2s$) and the threshold (dashed line). On the bottom are shown the detected frequencies (appearing as continuous because of the output signal amplitude remaining over the treshold for the whole signal duration time) and the theoretical frequency trend (dashed line).

a coefficient of data rejection for an ALE filter (APWGN noise only as input signal) of nearly 99% of the whole sample of 50 h of simulated data sampled at 1 kHz. The assumption we made for these tests was very simple, that is, we can have an alarm if the output signal is greater than the threshold T. During the 50^h run we got a total of 16 false alarms, whose duration was more or less of 1 or 2 msec: practically noise spikes. The conclusion, in our opinion is that the threshold we are using is very effective for the detection also taking into account the statistical procedure we have used to ascertain the significance of the output data (see next section).

VII. DETERMINATION OF THE ASTROPHYSICAL PARAMETERS OF COALESCING BINARIES

On the basis of the performances of the algorithms we implemented, we succeeded in separating the information coming from the input signals so that we tried to perform a *rough* estimate of the parameters of coalescence at the Newtonian order, i.e., trying to obtain the values of the mass parameter, $\mathcal{M}$, of the initial frequency, f_0, of the coalescence duration, τ and, finally, of the distance, d, in Mpc in the case of optimal orientation of the merging binary. We succeeded in obtaining the values of these parameters during the coalescence with an interval of confidence so that the range of physically meaningful parameters of the coalescence is greatly reduced and the problem of the huge demand of computing power required by the matched-filtering technique to work could be considered greatly reduced.

In connection with the data available [i.e., a reliable detection and estimate of the trend of the frequency and of the demodulated amplitude of the signal along the time, $f_0(t)$ and $h(t)$, respectively] for the full exploitation of the information they have embedded from the source, it is necessary to use a suitable algorithm of analysis that does not require an initial guess of the parameters. Therefore, among the several distinct subjects involved in the analysis of GW signals from coalescing binaries we propose a procedure to get the rough estimate of their parameters through the synthetized amplitudes and frequencies of the signal based on the controlled random search (CRS) by Price (1987) [66]. This is a global optimization algorithm, which represents a powerful extension of the simplex technique [66]. We want just to recall that we use this algorithm to solve the problem of light and radial velocity curve solutions of the Roche-based eclipsing binary model of Wilson [67–70], but the method

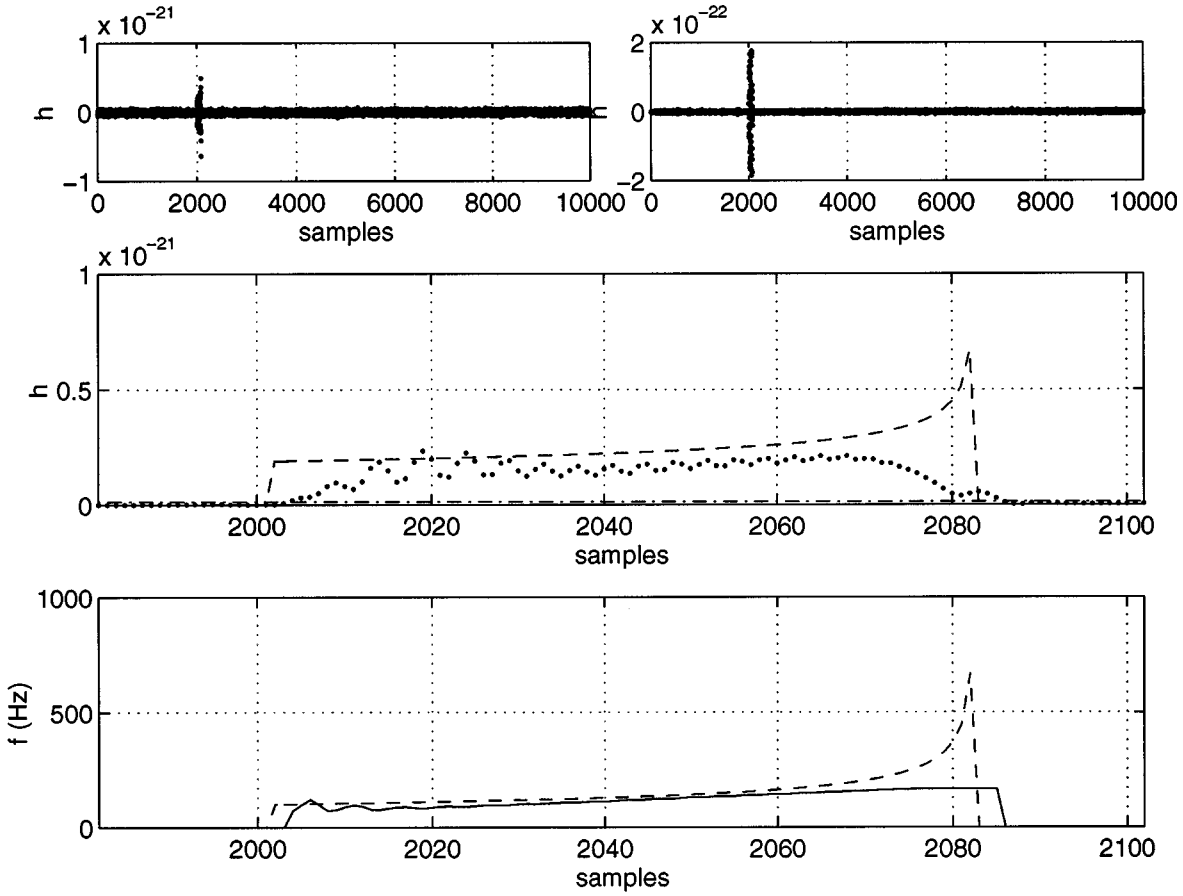

FIG. 6. From the top to the bottom clockwise: the GW input signal buried in noise, emitted by the classical NS-NS coalescing binary system of $(10.0-10.0M_{\odot})$ and coming from a distance of 500 Mpc (SNR$\approx+5$ dB) are shown. On the top right the output signal from ALE is shown. It is possible to see the great improvement of the $\mathrm{SNR}_{\mathrm{out}}$ that reach the value of $\approx+15$ dB. In the middle are shown the demodulated amplitude (dots), the theoretical one (continuous line, application time of the signal $2s$) and the threshold (dashed line). On the bottom are shown the detected frequencies (appearing as continuous because of the output signal amplitude remaining over the treshold for the whole signal duration time) and the theoretical frequency trend (dashed line).

can be easily applied to different problems like the one we are dealing with. In fact, a lot of problems, peculiar to the classical algorithms of data analysis, concerning the initial set of parameters, the uniqueness of the solution, and so on, can be avoided. We expose the fundamentals of the method in the Appendix.

To calibrate the procedure of optimization, we performed a rough analysis of the simulated data with the theoretical parameters shown in Table I. The input data for the CRS algorithm were established according to the following physical meaningful intervals: $0.25\leqslant K\leqslant 50$ search volume interval for the K parameter related to the chirp-mass $\mathcal{M}$; $(0.5\leqslant\mu\leqslant 6)M_{\odot}$ reduced mass search volume for PN1 only; $(2\leqslant M\leqslant 20)M_{\odot}$ total mass search volume for PN1 only; $70\leqslant f_0\leqslant 500$ Hz starting frequency search volume.

The distance was estimated from the demodulated amplitudes and the time evolution of the chirp frequencies according to the following formula:

$$\langle d\rangle=\frac{1}{n}\sum_{i=1}^{n}1.19\times10^{-22}\frac{K}{h(i)}f(i)^{2/3}. \tag{7.1}$$

In order to avoid problems of transient phases and taking into account the way of working both of ALE and of the amplitude envelope demodulator, for the rough estimate of the distance we discarded 10% of the initial and final data, both in frequency and demodulated amplitude. According to these limits we got the results shown in Table I. The average Price algorithm iteration number required for a solution was of 30 000 (this means a time of about 20 min off-line computation on an Alpha Vax).

In Figs. 7–9 it is possible to see the results we got from the analysis of the coalescence parameters for the detected systems shown before. In each figure (from the top to the bottom) the histogram of the distribution of the mass parameters obtained by Price algorithm, a normality test for the observed $\mathcal{M}$ distribution and, finally, a confidence ellipse at the two σ level for f_0 versus $\mathcal{M}$ are shown. The principal axes of the ellipse are, respectively, two standard deviations in $\mathcal{M}$ and two standard deviations in f_0. Using the Price algorithm, we got the estimates of the parameters of the coalescence, at the Newtonian order, from the detected signals with relative errors for the greater part of the systems less than 10% with respect to the theoretical values of the mass parameters (see Table I). The maximum relative error, $\approx$34%, is related to the lowest mass parameter (i.e., for $\mathcal{M}_t=0.44$). The distances were estimated obtaining relative errors less than 20%. It is now interesting to compute the

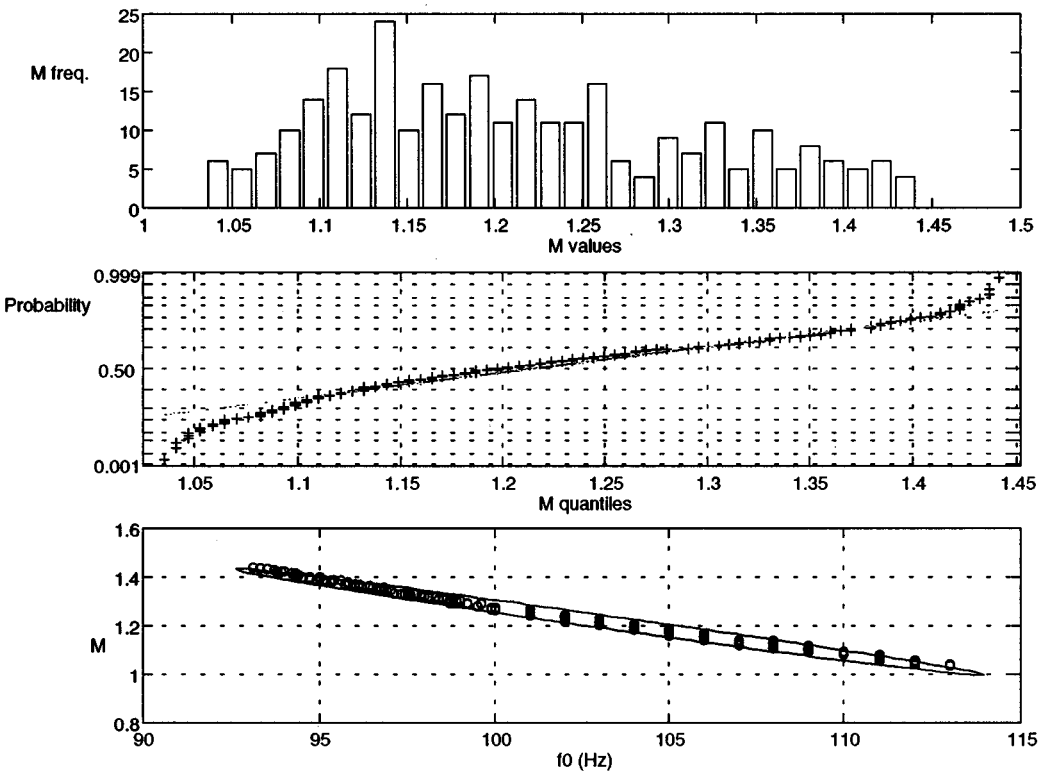

FIG. 7. From the top to the bottom for the NS-NS coalescing binary (1.4+1.4) system at 500 Mpc the output distribution of the computed mass parameters of the binary by the Price algorithm (top), normality test for the computed mass parameters, $\mathcal{M}$ (middle), the 95% confidence ellipse for the parameters solution $\mathcal{M}$ and f_0 (bottom) are shown.

gain in terms of computing power if we apply the matched-filtering technique as a refinement step of this hierarchical procedure. If we assume a range of uncertainty for the mass parameter equal to 50% (to be conservative) and apply the results of [48,49], it is easy to see that for the worst case (the first system reported in Table I) the computing power is decreased by a factor 10 (few GFlops are needed), while for the best case (the last system reported in Table I) only a few tens of MFlops are necessary.

To test the statistical significance of the results we obtained, we devised the following procedure. We generate a chunk of data constituted by noise only, having the same estimated duration of the simulated signal and we fed ALE with this *signal*. We performed the Price optimization using the so-obtained output frequencies. We got a set of parameters and we performed a *t*-Student test between the set of parameters obtained from the suspected signal and the pure noise signal one. We performed a two-tail null-hypothesis test using *t*-Student statistics for the mean at the level of significance 5% to verify if the samples of mass parameters obtained from the simulated signals could be extracted from the same population of the mass parameters obtained from a pure noise signal. As an example we tested a system of $(1.4-10)M_{\odot}$ whose theoretical value K_t is equal to 6.20, obtaining for the signal $K_s=6\pm1$ and for the pure noise signal $K_n=3.90\pm0.02$. Performing the *t*-Student test we can reject the null hypothesis at the level of significance both of 5% and 1%, so the difference is highly significative. This fact means also that the procedure we have devised is robust enough against false signals.

In this way we have statistically tested the whole procedure including an ALE plus Price algorithm. In Table I the duration of the coalescence estimated from the demodulated amplitudes are also shown. In Figs. 10 and 11 the results of the ALE detection and of the CRS astrophysical analysis for the classical $1.4-1.4M_{\odot}$ binary neutron stars system at the first post-Newtonian order for a distance of 300 Mpc are shown. The results we got for the worst case of noise environment, i.e., $\tilde{h}=2.10^{-21}$ Hz$^{-1/2}$ at 100 Hz are practically the same as for the optimistic case apart from the scaling of the limit distance of detection that undergoes a scaling factor 100 in respect of the optimistic sensitivity case. As it is possible to see, the results for the detection are similar to the ones at PN0. This fact means that with our procedure we can also analyze signals at post-Newtonian order, getting results useful to a more refined analysis. We tried to perform a direct estimate both of the reduced mass μ and of the total mass M. We got got $\mu=1.7\pm0.8$ in respect to a $\mu_t=0.7$ and $M=2.1\pm1.0$ in respect to $M_t=2.8$. In this case the results are not very encouraging but, for the solution we used only the *observed frequencies*.

VIII. CONCLUSIONS

We have shown in this paper a procedure for the rough on-line analysis which has allowed us to obtain the following results.

(a) We tested a very simple adaptive filter of practically negligible computational complexity: *the implementation of a single ALE requires 30 arithmetic operations*. This class of

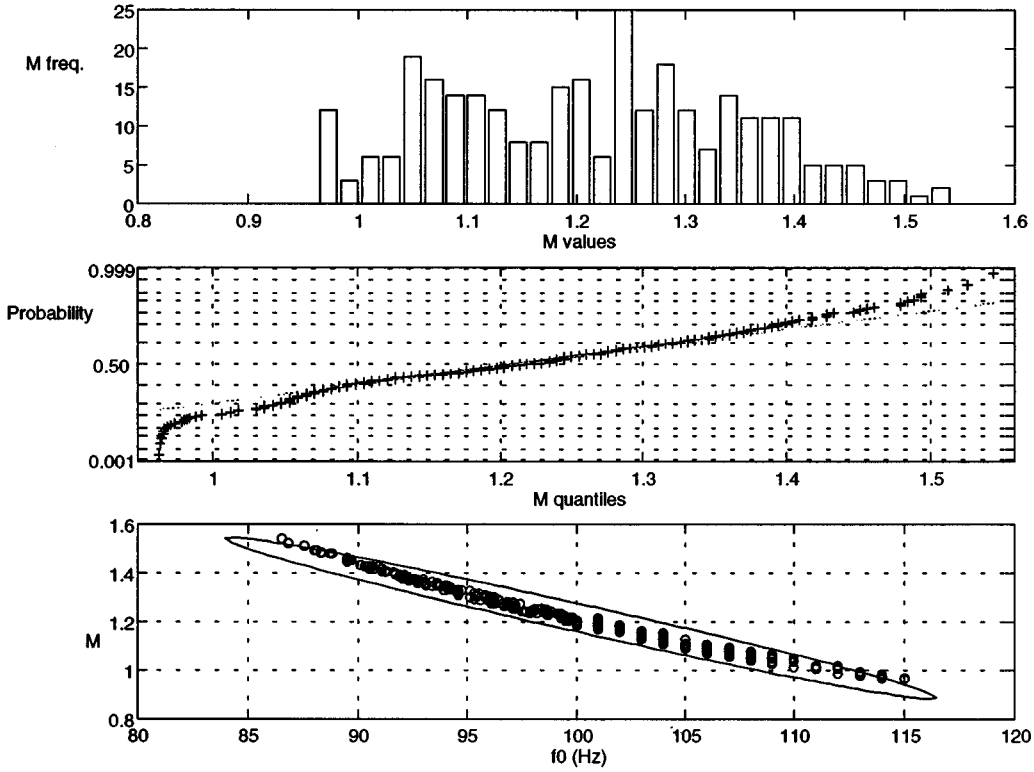

FIG. 8. From the top to the bottom for the NS-NS coalescing binary $(1.4+1.4M_{\odot})$ system at 100 Mpc, the output distribution of the computed mass parameters of the binary by the Price algorithm (top), normality test for the computed mass parameters, $\mathcal{M}$ (middle), the 95% confidence ellipse for the parameters solution $\mathcal{M}$ and f_0 (bottom) are shown.

filters can be easily used on-line with performances that are very interesting and effective taking care of the problems of misadjustment.

(b) We recall the attention of the interested reader to the results that are shown in Figs. 4–11. In our opinion they surely represent a fairly good and interesting solution to the problem of on-line data analysis for the class of coalescing binary signals: using the ALE coupled with the Price algorithm we can completely characterize the signal because we have two sources of information concerning both the trend of the frequency and of the amplitude evolution of the coalescence signal in the time domain with input SNR ratios that can also be of the order of 0.2. The conclusion is that an on-line rough and fast estimation of the parameters of the coalescence is possible and in any case useful to perform the initialization of more powerful refined analysis even on line. In fact, in our simulations we restricted the intervals of possible mass parameters so that the computational power demand for a matched filter is lowered at a level that could be a feasible on-line analysis by a parallel computer.

(c) This approach suggested for the analysis of GW coalescing binary signals could represent a good contribution towards the implementation of a fairly good approximation of a matched-filtering technique, without the necessity of huge computing power and overall without the need of an almost *exact* knowledge of the signal waveform. In fact, if we apply a hierarchical procedure using the results we reported in Table I using the results obtained with ALE to be refined with a matched-filtering technique, we reduce the computing power needed by a factor 10 for the worst case (first system in Table I) and to few tens of MFlops for the best case (last system in Table I).

Certainly there are, at the moment, limits and drawbacks of this procedure. Great relevance assumes the problem of missing the final part of the coalescence owing to the strong frequency gradient. This fact means that we must correct the adaptation step size of the filter so that the gradient μ_a can be adaptively increased at the increase of the output frequency, taking full care of the filter stability problems. It is also worth noticing the noise environment we used for the simulation. Of course, we are well aware that we must assume in the future a more realistic noise model: we must also test the robustness of the filter against interference, like thermal pendular resonances that are surely present in the sensitivity curve of LIGO and VIRGO antennas. The robustness can be achieved using adaptive notch filter like the ones used for the tracking of the signal, but permitting only a moderate excursion in an assigned frequency band in such a way to also take account of small parametric variations of the resonances due to different unpredictable sources of noise.

Last but not the least, we must perform a more complete and accurate test of statistical significance of the algorithm. In a following paper we shall accomplish all these tasks using also more refined signal forms [47], but we are confident in succeeding in finding reasonable solutions to the remaining problems both for ALE and for the Price algorithm.

APPENDIX

We give, now, a brief outline of CRS (for further details, see [66]). Given a function f of m variables whose minima have to be found, one has to assign limits to each of the m

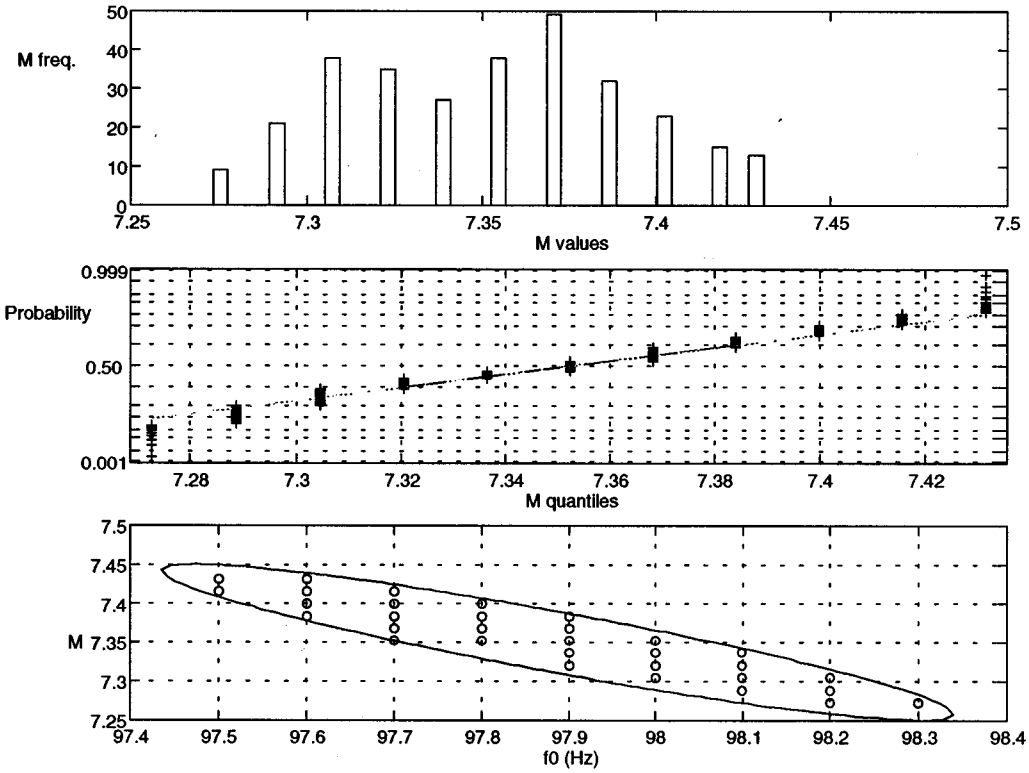

FIG. 9. From the top to the bottom for the NS-NS coalescing binary $(10.0+10.0M_{\odot})$ system at 500 Mpc, the output distribution of the computed mass parameters of the binary by the Price algorithm (top), normality test for the computed mass parameters, $\mathcal{M}$ (middle), bottom the 95% confidence ellipse for the parameters solution $\mathcal{M}$ and f_0 (bottom) are shown.

variables thus defining an initial search volume V. Hence the minimization procedure can be expressed by

$$S_{\rm sol}=\mathrm{MIN}[f(x_1,x_2,\ldots,x_m)], \tag{A1}$$

where $(x_1,x_2,\ldots,x_m)\in V$, i.e.,

$$x_{1_{\rm low}}\leqslant x_1\leqslant x_{1_{\rm up}},\quad x_{2_{\rm low}}\leqslant x_2\leqslant x_{2_{\rm up}},\quad x_{m_{\rm low}}\leqslant x_m\leqslant x_{m_{\rm up}}. \tag{A2}$$

A number N of trial points is randomly chosen within this domain, consistent with the constraints. The coordinates of every point and the function values are stored in an $N\times(m+1)$ array A whose structure is

$$\begin{pmatrix} x_{11} & x_{12} & \cdots & x_{1m} & f_1 \\ x_{21} & x_{22} & \cdots & x_{2m} & f_2 \\ \cdots & \cdots & \cdots & \cdots & \cdots \\ x_{m1} & x_{m2} & \ldots & x_{mm} & f_m \end{pmatrix}. \tag{A3}$$

After this initialization step, the real minimization procedure begins. A trial point P is selected in a way that depends on the points stored in the array A. In $m+1$ points $(R_1,R_2,\ldots,R_{m+1})$ are randomly extracted from the array and the centroid G of the first m points $(R_1,R_2,..,R_m)$ is evaluated. Then the trial point P is determined following the algebraic operation

$$P=2\cdot G-R_{m+1}. \tag{A4}$$

If the value of the function in P is less than the maximum value stored in A, then P replaces this point, otherwise a new trial point is selected. The algorithm iterates within this scheme. The set of N points of A tends to cluster around the minima, as shown by Price (1976) [66], but can (randomly) reach also zones far from detected minima (a useful feature to get out of the local ones).

The higher the number of lines of the array A, the higher is the probability of finding a global minimum. The higher the number of iterations, the better the definition of minima. The algorithm does not specify a particular stop criterion, leaving the choice to the user, but we studied the property of convergence in probability of this procedure and established a suitable stop criterion using the results of a study reported in the next paragraph.

1. Convergence of the Price algorithm

The convergence of the Price algorithm can be shown, in a heuristic way, assuming that the objective function is continuous in the search volume V and that there is a unique global minimum (this last hypothesis is assumed for sake of simplicity but is not strictly necessary).

The generation of the grid in the search volume gives a sample of a uniform stochastic variable of dimension 1. At each iteration, the new generated point can expressed as follows:

$$P_s=\frac{1}{2}\left(\frac{2}{m}\cdot\sum_{i=1}^{m_f}P_i-2\cdot R_{m+1}\right). \tag{A5}$$

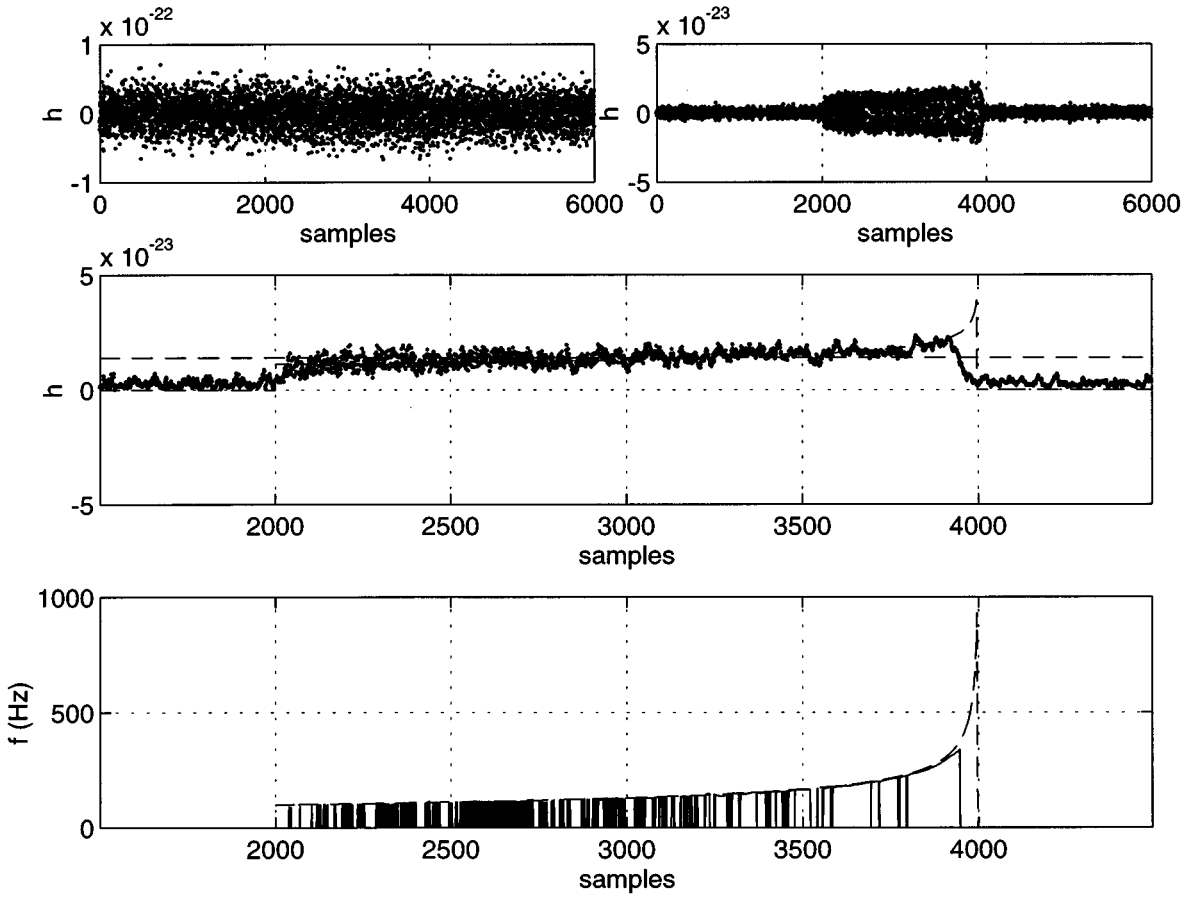

FIG. 10. Detection of the GW signal from the classical $(1.4+1.4M_{\odot})$ binary neutron star coalescence at a distance of 300 Mpc at PN1 order. Clockwise from the top left to the bottom the signal buried in noise (SNR$\approx$0 dB), the detected output signal from ALE top right are shown. In the middle the detected demodulated amplitude (dots) and the theoretical one (dashed line) together with the threshold are shown. In the bottom the detected frequencies (bars) and their theoretical trend (dashed line) are shown.

From Eq. (A5) we can deduce that P_s is the sample mean of the stochastic variables: $2/m\cdot\Sigma_{i=1}^{m_f}P_i$ and $-2\cdot R_{m+1}$ and both have finite variances owing to the fact the the first one is the sample mean of m stochastic variables extracted from a uniform distribution according to the hypothesis we made, while the second one because it is extracted from a uniform distribution. So the new generated point will be a stochastic variable extracted from a finite variance distribution. After k iterations, each stochastic variables, $P_i(i=1,\ldots,m+1)$, involved in the process of generation of the new point tends to be a sample mean. This means that the stochastic process fulfills the hypothesis of the central limit theorem and so we can affirm that the distribution of the grid points will tend to a Gaussian distribution with increasing the number of iterations. The mean of this distribution will be coincident with the global minimum, if the dimension m of the grid is large enough.

First of all let us demonstrate that the distribution variance decreases with the increasing of the iterations: at the kth iteration, being f_{m_k} the maximum of the objective function, f, over the grid points, P_s the new generated point, let us define

$$p_k=\mathrm{Prob}[f(P_s)<f_{m_k}]. \tag{A6}$$

If k is great enough, the point grid distribution will no longer be uniform; this fact implies that some zones of the search volume will not be reachable starting from the grid points (there will not be a simplex from which a reflection alone would be possible to generate whatever point of the grid as at the beginning of the process) so we have

$$p_k\leqslant\frac{\mathrm{meas}(\{P:f(P)<f_{m_k}\})}{\mathrm{meas}(V)}=p_{m_k}. \tag{A7}$$

The equal sign on the left-hand side of the disequation is true only in the case of the possibility of a complete exploration of the whole search volume, starting from whatever point of the grid. If m is great enough this fact happens until to a number of iterations k such that we are guaranteed a reasonably complete scanning of the search volume V (the greater m, the greater is the completeness of the scanning). At the $(k+1)$th iteration we could have one of the following cases:

(1) $f(P_s)<f_{m_k}\Rightarrow f_{m_{k+1}}<f_{m_k}\Rightarrow p_{m_{k+1}}<p_{m_k}$,

(2) $f_{m_k}\leqslant f(P_s)\Rightarrow f_{m_{k+1}}=f_{m_k}\Rightarrow p_{m_{k+1}}=p_{m_k}$.

This implies that

(3) $(\lim_{k\to\infty}p_{m_k}=0)\Rightarrow(\lim_{k\to\infty}p_k=0)$.

Be P_l the lth point for which we will have that the limit condition is fulfilled: the choice of a new point P_s depends only on the grid configuration, so if the variance of the dis-

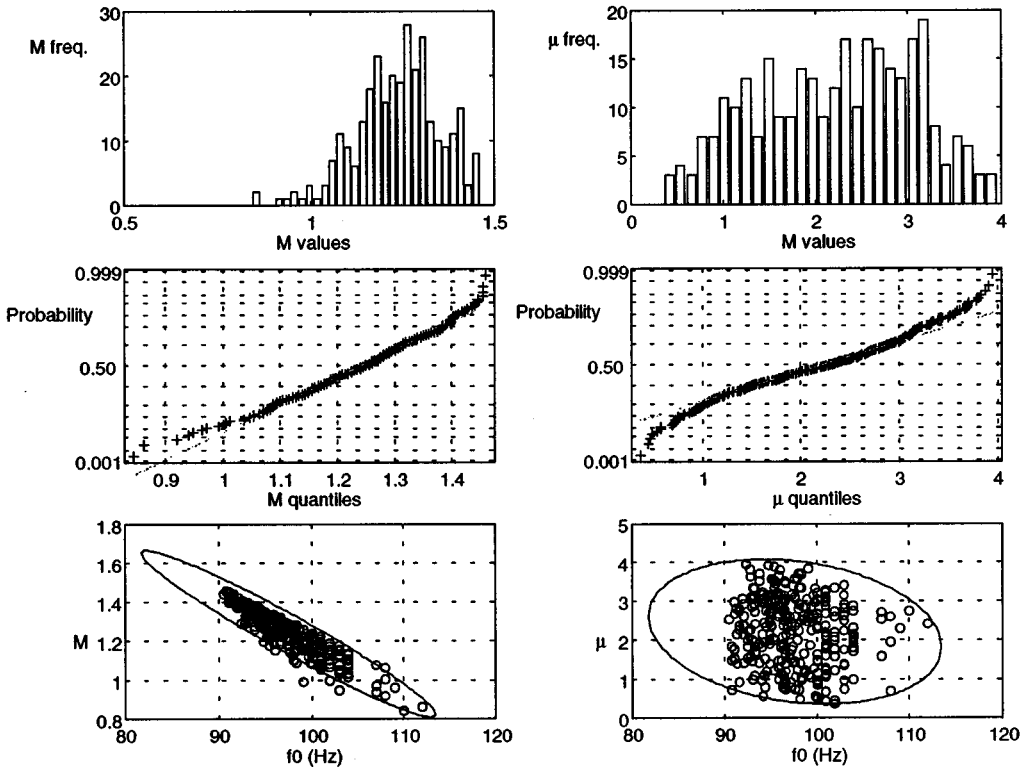

FIG. 11. Statistical analysis of the results we got from Price algorithm for the parameters at PN1 order for the parameters of the binary shown in Fig. 10. In this figure only the results for the mass parameter $\mathcal{M}$, the frequency f_0, and the reduced mass μ are shown.

tribution would not decrease then the conditions written above would not be verified. In the ideal case the conditions will be asymptotically satisfied ($k\rightarrow\infty$), and this means that we will never have null variance. Actually the points of the search volume belong to a grid, whose step can be, in the best case, equal to the physical limit imposed by the machine precision of the computer used. Therefore, defining such step d, we will have *convergence over the point* when

$$\sigma_i^2 \leqslant d^2, \quad i=1,2,\ldots,m, \tag{A8}$$

where σ_i^2 is the variance of the ith parameter. In this situation, the grid points will collapse all on the point P_l, or, more precisely, on the nearest grid point. When this situation is verified we will definitively have $P_k=P_l$ because the generation of points different from P_l will no longer be possible. If at this stage the mean of the points distribution were not a minimum, or if it were not a point of global minimum, this would imply the existence of at least a point P' different from P_l such that $f(P')<f(P_l)$. The existence of such a point is guaranteed by the continuity of the function, but conditions (1) and (2) and consequence (3), written above, state that waiting for a number of iterations k great enough, the probability of the occurrence of that kind tends to zero. Therefore, we have heuristically demonstrated the convergence in probability of the Price algorithm. The practical consequences of the above conclusions are that all the information, coming from Price algorithm, could be expressed by a quality coefficient, which quantifies the goodness of the fitting and, at the same time, represents the connection between the mathematics and the physics of the solution procedure. The structure of such a coefficient must be a balanced synthesis of different aspects of the problem and must give precise information on the following two items.

(1) The validity of the physical model used on the basis of the type, the quality and the quantity of data available. In practice, it is important to verify which are the physical phenomena whose presence can be ascertained only on the basis of the data and, as consequence, the type and the number of parameters which correctly describe the system.

(2) The level of significance of the solutions preventing us from the false alarm probability at a fixed level of confidence. In the hypothesis of a correct description of the system, it should also permit one to quantify the errors on each physical and geometrical parameter. An obvious choice for this quality index S comes from fitting the data in the least squares sense, i.e., minimizing the value of the function (in the general case in which the GW frequency and amplitude curves are solved together)

$$S=\frac{1}{n_f}\sum_{i=1}^{n_f} wf_i(f_{i,\mathrm{obs}}-f_{i,\mathrm{comp}})^2 + \frac{1}{n_h}\sum_{l=1}^{n_h} wh_l(h_{l,\mathrm{obs}}-h_{l,\mathrm{comp}})^2, \tag{A9}$$

where wf_i and wh_l are the weights of the points of frequency and amplitude curves, n_f, n_h are the number of observations in each curve, respectively. At this point it is evident that the quality index S we have introduced is proportional to the statistic χ^2, assuming that the final distribution of the param-

eters is Gaussian as we have heuristically demonstrated above. On the basis of what was said above, the determination of statistically meaningful solutions can be synthetized in the following procedure.

We assume that the physical model used can exactly fit the *noise free* observations and that the estimated standard deviation $\hat{\sigma}$ is correctly calculated. We choose a value $l=0.50$ as a level of significance for the solutions and calculate the value of $S_{0.50}$ which corresponds to a value of the probability distribution function $P_{\chi}(\chi,\nu)=0.50$ and is indicative of a good fit: all the solutions characterized by $S\leqslant S_{0.50}$ are statistically meaningful solutions at least at the level of significance 0.50 and must be stored during the minimization procedure. Then it is necessary to ascertain that the global minimum is characterized by a value of the order of $S\approx S_{0.50}$, that is indicative of a good fit. If this hypothesis is verified then it is necessary to build a large set of solutions characterized by $S\leqslant S_{0.50}$, using also the previously stored ones. This set permits one to calculate the parameters and the relative errors by simply evaluating the mean and standard deviation of the parameters of the stored solutions.

Concerning the CPU time required for a solution we can say that it depends, of course, on the time required for each iteration by the objective function computation and on the number of iterations. Because of the (controlled) random search used, a new iteration does not necessarily update the search array. Therefore, the number of iterations may be very high, but in our case the objective function requires a very low time of computation per iteration so the algorithm could work on line.

[1] C.W. Misner, K.S. Thorne, and J.A. Wheeler, *Gravitation* (Freeman, San Francisco, 1973).

[2] D.G. Blair, *The Detection of Gravitational Waves* (Cambridge University Press, Cambridge, England, 1991).

[3] P.R. Saulson, *Fundamentals of Interferometric Gravitational Wave Detectors* (World Scientific, New Jersey, 1994).

[4] J. Weber, Phys. Rev. **117**, 306 (1960).

[5] M. Bassan, Class. Quantum Grav. **39**, 11 (1994).

[6] R. Weiss, Q. Prog. Rep. RLE, MIT, **105**, 54 (1971).

[7] G.E. Moss, L.R. Miller, and R.L. Forward, Appl. Opt. **10**, 2495 (1971).

[8] J.W. Armstrong, F.B. Estabrook, and H.D. Walquist, Astrophys. J. **318**, 536 (1987).

[9] P. Bender, I. Ciufolini, J. Cornelisse, K. Danzmann, W. Folkner, F. Hechler, J. Hough, Y. Jafry, R. Reinhard, D. Robertson, A. Rüdiger, M. Sandford, R. Schilling, B. Schutz, R. Stebbins, T. Summer, P. Toubol, S. Vitale, H. Ward, and W. Winkler, ''LISA: Laser Interferometer Space Antenna for the detection and the observation of gravitational waves,'' ESA Report No. MPQ 208, 1996 (unpublished).

[10] R.A. Hulse and J.H. Taylor, Astrophys. J. **195**, L51 (1975).

[11] J.H. Taylor and J.M. Weisberg, Astrophys. J. **345**, 434 (1989).

[12] J.H. Taylor, Rev. Mod. Phys. **66**, 253 (1994).

[13] J. Hough *et al.*, ''Proposal for a joint German-British Interferometric Gravitational Wave Detector,'' Max Planck Institut Report No. MPQ 147, 1989 (unpublished).

[14] A. Abramovici *et al.*, Science **256**, 325 (1992).

[15] TAMA (unpublished).

[16] C. Bradaschia *et al.*, Nucl. Instrum. Methods Phys. Res. A **289**, 518 (1990).

[17] J.P.A. Clark, E.P.J. van den Heuvel, and W. Sutantyo, Astron. Astrophys. **72**, 120 (1979).

[18] E.S. Phinney, Astrophys. J. **380**, L17 (1991).

[19] R. Narayan, T. Piran, and A. Shemi, Astrophys. J. **379**, L17 (1991).

[20] A.V. Tutukov and L.R. Yungelson, Mon. Not. R. Astron. Soc. **260**, 675 (1993).

[21] B.S. Sathyaprakash and S.V. Dhurandar, Astrophys. J. **44**, 3819 (1991).

[22] B.F. Schutz, Class. Quantum Grav. **6**, 1761 (1989).

[23] B.F. Schutz, Class. Quantum Grav. **10**, S135 (1993).

[24] K.S. Thorne, in *300 Years of Gravitation*, edited by S.W. Hawking and W. Israel (Cambridge University Press, Cambridge, England, 1970), p. 330.

[25] K.S. Thorne, in *Fourth Rencontres de Blois*, edited by G. Fontaine J. Tran Thanh Van (Edition Frontíeres, France, 1993).

[26] K.S. Thorne, in *8th Nishinomiya-Yukawa Symposium on Relativistic Cosmology*, edited by M. Sasaki (Universal Academic Press, Japan, 1994), p. 67.

[27] A. Królak and B.F. Schutz, Gen. Relativ. Gravit. **19**, 1163 (1987).

[28] A. Królak, in *Gravitational Wave Data Analysis*, edited by B.F. Schutz (Kluwer Academic, Dordrecht, 1989).

[29] C.W. Lincoln and C.M. Will, Phys. Rev. D **42**, 1123 (1990).

[30] C. Cutler, T.A. Apostolatos, L. Bildsten, L.S. Finn, E. Flanagan, D. Kennefick, D.M. Markovix, A. Ori, E. Poisson, G.J. Sussman, and K.S. Thorne, Phys. Rev. Lett. **70**, 2984 (1993).

[31] L.S. Finn and D.F. Chernoff, Phys. Rev. D **47**, 2198 (1993).

[32] C. Cutler and E. Flanagan, Phys. Rev. D **49**, 2658 (1994).

[33] E. Poisson and C.M. Will, Phys. Rev. D **52**, 848 (1995).

[34] A. Królak, K.D. Kokkotas, and G. Schäfer, Phys. Rev. D **52**, 2089 (1995).

[35] K.S. Thorne (unpublished).

[36] K.S. Thorne, in *First International LISA Symposium*, Chilton, Oxfordshire, England, 1996, edited by M.C.W. Sandford (in press).

[37] C.W. Helstrom, *Statistical Theory of Signal Detection*, 2nd ed. (Pergamon, London, England, 1968).

[38] A. Papoulis, *Signal Analysis* (McGraw-Hill, Singapore, 1984).

[39] S.V. Dhurnadhar and B.S. Sathyaprakash, Phys. Rev. D **49**, 1707 (1994).

[40] C.M. Will, in *8th Mishinomiya-Yukawa Symposium on Relativistic Cosmology*, edited by M. Sasaki (Universal Academic Press, Japan, 1994), p. 83.

[41] L. Blanchet, T. Damour, and B.R. Iyer, Phys. Rev. D **51**, 5360 (1995).

[42] C.M. Will and A.G. Wiseman (in preparation).

[43] L. Blanchet, T. Damour, B.R. Iyer, and A.G. Wiseman, Phys. Rev. Lett. **74**, 3515 (1995).

[44] L. Blanchet report, 1996 (unpublished).

[45] C. Cutler, L.S. Finn, E. Poisson, and V.I. Sussman, Phys. Rev. D **47**, 1511 (1993).

[46] E. Poisson, Phys. Rev. D **52**, 5719 (1995).
[47] L. Blanchet, B.R. Iyer, C.M. Will, and A.G. Wiseman, Class. Quantum Grav. (to be published).
[48] M. Beccaria, G. Cella, A. Ciampa, E. Cuoco, G. Curci, and A. Viceré, Virgo Report No. NTS96-024, 1996 (unpublished).
[49] R. Owen (unpublished).
[50] S. Smith, Phys. Rev. D **36**, 2901 (1987).
[51] S.D. Mohanty and S.V. Dhurandhar, ''Virgo Data Analysis Meeting,'' Virgo Report No. NTS 96-39, 1996 (unpublished).
[52] X. Grave, F. Marion, R. Morand, B. Mours, F. Barone, F. Garufi, L. Milano, G. Russo, F. Cavalier, M. Davier, F. Le Diberder, and P. Roudier, in *International Conference on Gravitational Waves: Sources and Detectors*, edited by A. Di Giacomo (Cascina, Pisa, 1996).
[53] F. Barone, E. Calloni, L. Di Fiore, A. Grado, L. Milano, and G. Russo Rev. Sci. Instrum. **67**, 4353 (1995).
[54] L. Milano, F. Barone, E. Calloni, A. Grado, and L. Di Fiore, in *International Conference on Gravitational Waves: Sources and Detectors* [52].
[55] L. Milano, F. Barone, and M. Milano, in *First International Lisa Symposium* [39].
[56] R.V. Raja and R.N. Pal, IEEE Trans. Acoust. Speech Signal Process. **38**, 1710 (1990).
[57] D. Verkindt, Ph.D, these, Universitéde Savoie, 1993.
[58] S.V. Dhurandar and M. Tinto, Mon. Not. R. Astron. Soc. **234**, 663 (1988).
[59] Y. Gursel and M. Tinto, Phys. Rev. D **40**, 3884 (1989).
[60] B. Widrow and S. Stearns, *Adaptive Signal Processing* (Prentice Hall, New Jersey, 1985).
[61] S. Orfanidis, *Optimum Signal Processing* (MacMillan, New York, 1985).
[62] N. Bershad and P. Feintuch, IEEE Trans. Acoust. Speech Signal Process. **28**, 652 (1980).
[63] J.R. Zeidler *et al.*, IEEE Trans. Acoust. Speech Signal Process. **26**, 240 (1978).
[64] J. Rickard, J. Zeidler, M. Dentino, and M. Shensa, IEEE Trans. Acoust. Speech Signal Process. **29**, 694 (1981).
[65] J.R. Treichler, IEEE Trans. Acoust. Speech Signal Process. **27**, 53 (1979).
[66] W.L. Price, Comput. J. (UK) **20**, 367 (1976).
[67] R.E. Wilson and E.J. Devinney, Astrophys. J. **166**, 605 (1971).
[68] F. Barone, L. Milano, G. Russo, Mem. Soc. Astron. Ital. **59**, 3 (1987).
[69] F. Barone, C. Maceroni, L. Milano, and G. Russo, Astron. Astrophys. **197**, 347 (1988).
[70] F. Barone, L. Di Fiore, L. Milano, and G. Russo, Astrophys. J. **407**, 2037 (1993).